



## Investigation of Histological and Histochemical Features of Mouse Placenta in Different Periods of Pregnancy \*

Seçil KOÇ<sup>1,a</sup>, Şadiye KUM<sup>2,b,\*\*</sup>

<sup>1</sup>Aydın Adnan Menderes University, Institute of Health Sciences, Department of Histology and Embryology, Aydın, Türkiye.

<sup>2</sup>Aydın Adnan Menderes University, Department of Histology and Embryology, Faculty of Veterinary Medicine, Aydın, Türkiye.

<sup>a</sup> ORCID: 0000-0002-9228-4682

<sup>b</sup> ORCID: 0000-0001-6586-4596

Received: 05.10.2023

Accepted: 31.10.2023

**How to cite this article:** Koç S, Kum Ş. (2023). Investigation of Histological and Histochemical Features of Mouse Placenta in Different Periods of Pregnancy.

Harran Üniversitesi Veteriner Fakültesi Dergisi, 12(2):166-179.

DOI:10.31196/huvfd.1371723.

**\*Correspondence:** Şadiye Kum

Aydın Adnan Menderes University, Department of Histology and Embryology, Faculty of Veterinary Medicine, Aydın, Türkiye.

e-mail: skum@adu.edu.tr

Available on-line at: <https://dergipark.org.tr/tr/pub/huvfd>

**Abstract:** This study aimed to investigate the histological and histochemical properties of mouse placenta samples from different periods of pregnancy. For this purpose, mouse placenta samples were collected on the fourth, tenth, and seventeenth days of pregnancy and blocked in paraffin. Serial sections of 5µ thickness were taken at 50µ intervals. Histological and histochemical staining methods were applied to the sections. As a result, histological and histochemical characteristics of mouse placenta from different periods of pregnancy were determined.

**Keywords:** Histochemistry, Histology, Mouse, Placenta.

### Gebeliğin Farklı Dönemlerindeki Fare Plasentasının Histolojik ve Histokimyasal Özelliklerinin İncelenmesi

**Özet:** Bu çalışmada gebeliğin farklı dönemlerine ait fare plasenta örneklerinin histolojik ve histokimyasal özelliklerinin araştırılması amaçlanmıştır. Bu amaçla gebeliğin dördüncü, onuncu ve on yedinci günlerindeki fare plasenta örnekleri toplanarak parafinde bloklandılar. 50µ ara ile 5µ kalınlığında seri kesitler alındı. Kesitlere histolojik ve histokimyasal boyama yöntemleri uygulandı. Sonuç olarak gebeliğin farklı dönemlerine ait fare plasentasının histolojik ve histokimyasal özellikleri belirlendi.

**Anahtar kelimeler:** Fare, Histokimya, Histoloji, Plasenta.

## Introduction

Placenta; it is an extraembryonic tissue that creates an environment for the fetus to develop in the uterus and is found only in mammals. The placenta, which carries out the fetomaternal exchange of nutrients and substances during pregnancy, also serves as a comprehensive endocrine organ (Furukawa et al., 2011; Tewari et al., 2011).

Since developmental and experimental studies on the human placenta are not ethically possible, animal placentas are used as placenta models. The Mouse placenta is preferred as an animal model in many studies due to its phylogenetically similar structure to humans, ease of supply, suitability of pregnancy and cycle duration, and ease of animal care (Adams et al., 2020; Wu et al., 2018; Yu et al., 2018; Zhu et al., 2019).

The mouse placenta is a chorioallantoic type placenta and has a discoidal shape. Histologically, it is classified as hemotrichorial (Furukawa et al., 2011). It is also classified as hemoendothelial in some sources (Özer, 2007). The mature mouse placenta is fully formed in 10.5 days. It is shaped from three layers; 1. Labyrinth zone 2. Connection zone 3. Maternal decidua. It also contains a special membrane called Reichert's Membrane, which is unique to rodents (Chavatte-Palmer and Tarrade, 2016; Furukawa et al., 2014; Hafez, 2017; Johnson and Everitt, 2018; McGeady et al., 2017; Rai and Cross, 2014; Sinowatz, 2009).

This study aimed to investigate mouse placenta samples' histological and histochemical properties from the fourth, tenth, and seventeenth days of pregnancy.

## Material and Methods

In the present study, 21 female and 7 male mice of the CD-1 race, aged 8-10 weeks were used. The vaginal plug was checked every morning and the pregnant ones were placed in separate cages. Those with a positive vaginal plug were considered to be on the first day of pregnancy. Seven healthy mouse placentas were obtained as material from animals euthanized by cervical dislocation under ether anesthesia on the fourth, tenth, and seventeenth days of pregnancy. After the tissue materials were fixed in 10% neutral buffered formaldehyde for 24 hours, they went through routine tissue tracking stages and were embedded in paraffin. Serial sections of 5 $\mu$  thickness were taken from the prepared paraffin blocks at 50 $\mu$  intervals (Koç and Kum, 2022). Histological and histochemical staining methods (Table 1) were applied to the sections obtained from paraffin blocks. The obtained data were evaluated light microscopically (Leica DMLB, Made in Germany). For this study, permission was received from Aydın Adnan Menderes University Animal Experiments Local Ethics Committee (ADU HADYEK 64583101/2016/017).

**Table 1.** Applied staining methods and purposes of the methods.

METHOD	PURPOSE OF THE METHOD
Hematoksilen-Eozin (Culling et al, 1985)	Determination of general histological appearance
Triple Stain (Culling et al, 1985)	Determination of general histological appearance
Periyodik Asit-Schiff(PAS) (Culling et al, 1985)	Demonstration of neutral mucosubstance
Alcian Blue pH 2.5 (AB pH 2.5 )(Culling et al, 1985)	Determination of carboxylated acidic mucosubstance
PAS/AB pH 2.5 (Culling et al, 1985)	Coexistence of neutral and acidic mucosubstance
Aldehit Fuksin (AF) (Culling et al, 1985)	Determination of sulfated acidic mucosubstance
AB pH 1.0 (Culling et al, 1985)	Determination of O-sulfate ester mucosubstance
AB pH 0.5 (Culling et al, 1985)	Determination of strong sulfated mucosubstance
AF/AB pH 2.5 (Culling et al, 1985)	Coexistence of sulfated and carboxylated acidic mucosubstance

## Results

**Fourth day:** On the fourth day, it was observed that the histological structure of the uterus was preserved. The structure of the endometrium, myometrium, and perimetrium was generally normal (Figure 1A). No implantation was observed on the fourth day. It was observed that the structure and integrity of the epithelial cells in the endometrium lamina epithelium began to deteriorate in some places. It was observed that stromal cells were changed in the lamina propria (Figure 1B). It was observed that the cells that started to change often had more than one nucleolus. Cells containing vacuolar structures were found in the lamina propria and between epithelial cells. It was observed that the glands became small, and the structure of the gland epithelial cells and the

stroma around the glands changed. A large number of neutrophils were detected in the functional lamina propria of the endometrium. Again, in most samples, numerous capillary blood vessels were observed in the functional endometrium. Vascular structures arranged in a clear line were also seen at the end of the endometrium basalis.

The reactions observed with histochemical staining methods applied on the fourth day of pregnancy are given in Table 2.

Moderate PAS positivity was observed on the surface of the lamina epithelialis, basement membrane, and gland epithelial cells. At Alcian blue pH 2.5, a weak reaction was observed on the lamina epithelialis surface, gland epithelial surface, and serosa. PAS/AB pH 2.5 staining determined that the AB reaction was dominant on the lamina epithelialis and gland epithelial surface. AF staining revealed a strong,

sometimes moderate, and low-grade AF positive reaction on the epithelial surface (Figure 2A). A moderate reaction was observed on the surface of the gland epithelial cells (Figure 2B). A strong AF reaction was detected in the serosa (Figure 2C) and the vessel wall (Figure 2D). A moderate reaction was observed on the gland epithelial surface in AB pH 1.0 and 0.5

methods (Figure 3A). A strong reaction was detected in the serosa (Figure 3B). In the AF/AB pH 2.5 staining method, it was noted that the AB reaction was dominant on the surface of the lamina epithelialis and gland epithelium. In the serosa, AF and AB reactions were observed to be similar.

**Table 2.** Histochemical reactions on the fourth day of pregnancy.

	PAS	AB pH 2.5	PAS+AB	AF	AB pH 1.0	AB pH 0.5	AF+AB
Lamina epithelialis	(++)	(+)	AB	(++)	(+)	(++)	Mostly AB, some parts AF
Gland epithelium	(++)	(+)	-	(++)	(++)	(+)	AB
Stroma	(++)	-	-	(+++)	-	-	-
Vascular Wall	(++)	-	-	(+++)	-	-	-
Serosa	(++)	(+)	PAS	(+++)	(+++)	(+++)	AF, AB, AF/AB

None (-), Weak (+), Medium (++), Strong (+++).

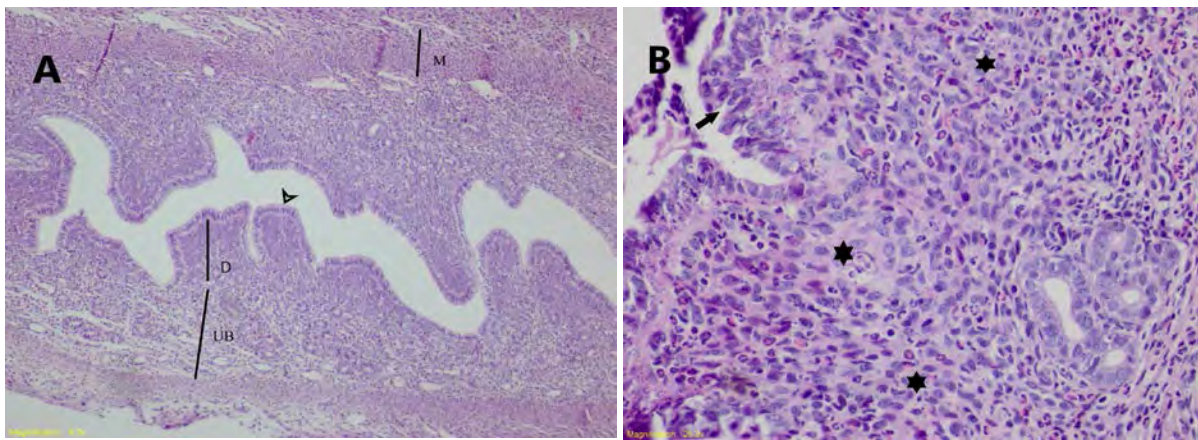


**Figure 1.** The fourth day of pregnancy. A. Lamina epithelialis (arrowhead), lamina propria part where cellular changes are seen (D), lamina propria where uterine glands are concentrated (UB), and myometrium (M). Hematoxylin-Eosin staining method. Bar 200 µm. B. Deterioration in epithelial integrity (arrow), changes in stroma cells (\*). Hematoxylin-Eosin staining method. Bar 50 µm.

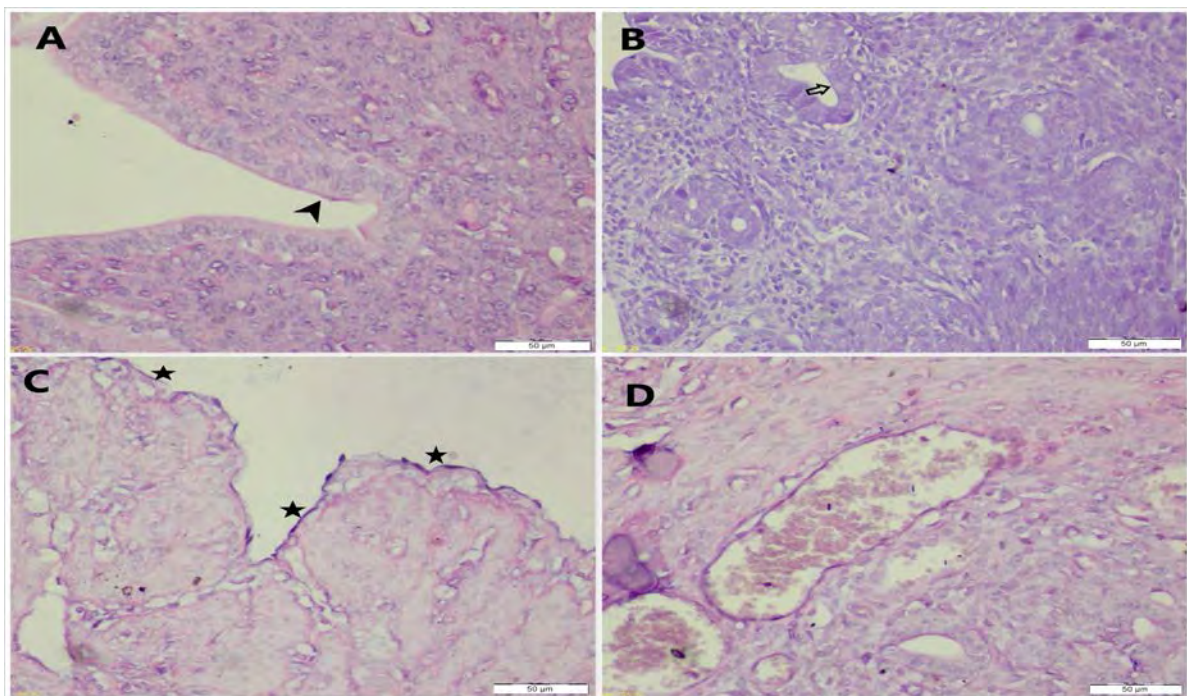


**Figure 2.** The fourth day of pregnancy. A) AF (+) reaction (arrowhead) on the lamina epithelialis surface. B) AF reaction observed on the surface of glandular epithelial cells (open arrow) C) AF (+) reaction on the serosal surface (\*). D) AF (+) reaction in the vessel wall. Aldehyde Fuchsin staining method. Bar 50 µm.

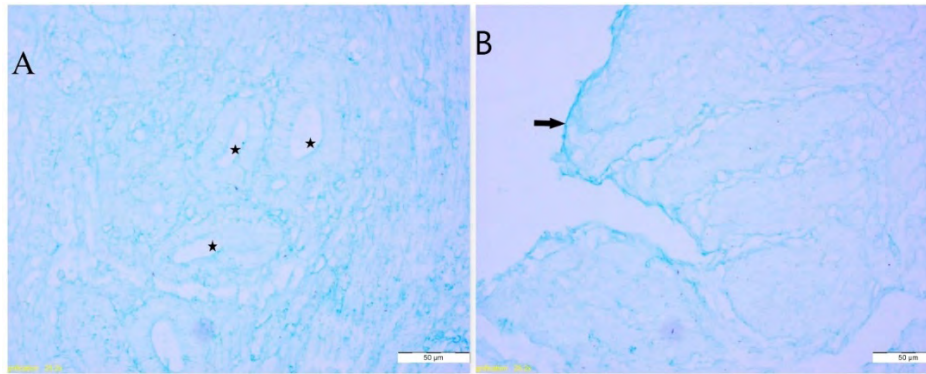


**Figure 3.** The fourth day of pregnancy. A) Moderate AB reaction on the glandular epithelial surface (\*). B) Strong AB reaction (arrow) in the tunica serosa. AB pH 1.0 staining method. Bar 50 µm.

**Tenth day:** On the tenth day, fetal and maternal structures could be clearly distinguished. The mesometrial and antimesometrial parts of the uterus were distinguished (Figure 4A). It was observed that the amniotic cavity grew noticeably and the amniotic membrane surrounded the fetus. It was observed that parietal trophoblastic giant cells (P-TGCs) surrounded the border of the entire amniotic cavity under the amniotic membrane. It was observed that the antimesometrium was much thinner than the mesometrium. In this section, as you move from the amniotic cavity towards the serosa; At first, single or several rows of trophoblastic giant cells (TGCs) were found in the amniotic membrane and the layer just below it (Figure 4B). Laterally, it was observed that P-TGCs began to separate into islets, their size increased compared to the antimesometrium, and blood pools began to be seen here and there between the islets. It was noted that there was a dense layer of antimesometrial decidua layer (decidua parietal) just below the P-TGCs (Figure 4B). The striking feature of antimesometrial decidua was the lack of vascularization. It was observed that vascularization increased towards the lateral and mesometrium. It was observed that the endometrial epithelium and its lumen were pushed between the antimesometrial decidua layer and the myometrium, and the lumen narrowed considerably (Figure 4B). It was observed that all these structures were surrounded by myometrium and perimetrium, respectively.

It was determined that the density of the decidua layer decreased and vascularization increased in the mesometrial section. It was observed that gaps began to form laterally between the decidua cells (Figure 5A). Structures belonging to the labyrinth of the placenta began to be seen under the amniotic membrane surrounding the amniotic cavity in the mesometrium (Figure 5B). Trophoblastic giant cells and syncytiotrophoblast (SynT) cell clusters were scattered. Maternal blood elements and fetal blood vessels were seen among these clusters. Fetal and maternal blood could be easily distinguished because fetal erythrocytes were darker stained and nucleated (Figure 5C, 5D). It was observed that there were several arranged and scattered trophoblast clusters around the fetal blood vessels. Maternal blood cells were located in irregular spaces in many parts of the labyrinth (Figure 5C, 5D).

Several cell layers, presumably a syncytiotrophoblast layer, were observed where the labyrinth zone ends. Following this layer, the P-TGC cell row was followed in a single or two rows. Laterally, P-TGCs were determined to be multi-row (Figure 6A, 6B). The main channel structure was observed just at the end of the labyrinth layer (Figure 6C). It was determined that the size of P-TGCs in the mesometrium was reduced compared to the antimesometrial and lateral ones. Following the P-TGCs sequence, a mesometrial decidua layer was observed up to the myometrium (Figure 6C, 6D). It was observed that spongiotrophoblast cells (SpTC) and glycogen cells (Gly-C) began to form in the decidua basalis just below the P-TGCs, and blood pools surrounded the cell groups. It was determined that SpTC was located in several rows just below the P-TGCs and the connection zone began to form here (Figure 6C, 6D, 6E, 6F). When examined from the connection zone towards the serosa, it was determined that decidua and Gly-C were fused and were not clearly distinguished. In the mesometrium, it was observed that decidua concentrated and Gly-C decreased. In a part close to the mesometrium, lymphocyte infiltrations were seen among the decidua tissue in the area called MLAp (Mesometrial lymphocyte community during pregnancy), separated by the myometrium (Figure 6G, 6H).

The reactions observed with histochemical staining methods applied on the tenth day of pregnancy are given in Table 3.

It was observed that the antimesometrium decidua cell borders became apparent with a medium-strength reaction with PAS (Figure 7A). While a medium-strength reaction was observed at the cell borders and the parts bordering the cell islets in the decidua basalis of the mesometrium, an extreme reaction was observed in the glycogen cells (Figures 7B, 7D). A granular PAS reaction was noted in the cytoplasm of glycogen cells (Figure 7C, 7D). In the AB pH 2.5 staining method, a weak reaction was observed in the uterine lumen in the antimesometrium, while a moderate reaction was observed in the serosa and lateral P-TGC. In the PAS/AB pH2.5 staining method, a large amount of PAS positivity was detected on the lamina epithelial surface in antimesometrium (Figure 8A). Although PAS positivity was mostly found in the serosa, reactions of similar intensity were observed (Figure 8B). PAS positivity was observed in

the junction zone glycogen cells and MLAp cells of the mesometrium (Figure 8C). In the labyrinth, PAS positivity was observed on the surface adjacent to the amniotic cavity, while AB positivity was observed in the stromal areas within the labyrinth (Figure 8D). In the aldehyde fuchsin staining method, reactions of different intensities were observed in the labyrinth, P-TGCs, and serosa. In the AB pH 1.0 staining method, a strong positive reaction was observed in the

serosa, and a moderate positive reaction in the decidua (Figure 9). The weak reaction was seen in glycogen cells and the labyrinth.

In the AB pH 0.5 staining method, a moderate reaction while in the labyrinth and a weak reaction in the glycogen cells of the decidua basalis was detected. In the AF/AB pH 2.5 staining method, AF positivity was detected in the antimesometrium and mesometrial serosa.

**Table 3.** Histochemical reactions on the tenth day of pregnancy,

	PAS	AB pH2.5	PAS+AB	AF	AB pH 1.0	AB pH 0.5	AF+AB
<b>Antimesometrial Decidua</b>	(++)	(Lamina epithelialis +)	PAS, PAS/AB	(++)	-	(++)	AF, AF/AB
<b>Antimesometrial P-TGC</b>	(+++) Granular	(++)	PAS	(++)	-	-	AF
<b>Mesometrial P-TGC</b>	(+++)	(++)	PAS	Reaction on the cell surface	(+)	(++)	AF
<b>Labyrinth</b>	(++)	(++)	AB	(++)	(+)	(++)	AF
<b>Mesometrial Decidua</b>	(++)	(++)	PAS	(++)	(++)	(+)	AF
<b>Glycogen Cells</b>	(+++) Granular	(++)	PAS	(++)	(+)	(++)	AF
<b>MLAp</b>	(+++)	(+)	PAS	(++)	(++)	(+)	AF
<b>Serosa</b>	(++)	(+)	PAS, PAS/AB	(++)	(++)	(++)	AF, AF/AB

None (-), Weak (+), Medium (++), Strong (+++).

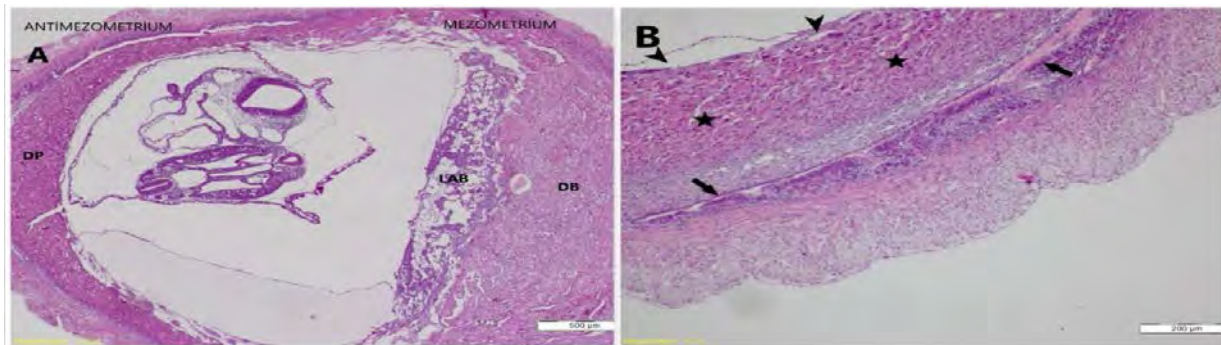


**Figure 4.** Tenth day of pregnancy. **A.** DP: Decidua parietalis, DB: Decidua basalis, LAB: Labyrinth. Bar 500 µm. **B.** Antimesometrial part of the uterus (decidua parietalis). P-TGC (arrowheads), decidua parietalis surrounding the amniotic cavity (\*), endometrium lamina epithelialis (arrows). Hematoxylin-Eosin staining method. Bar 200 µm.

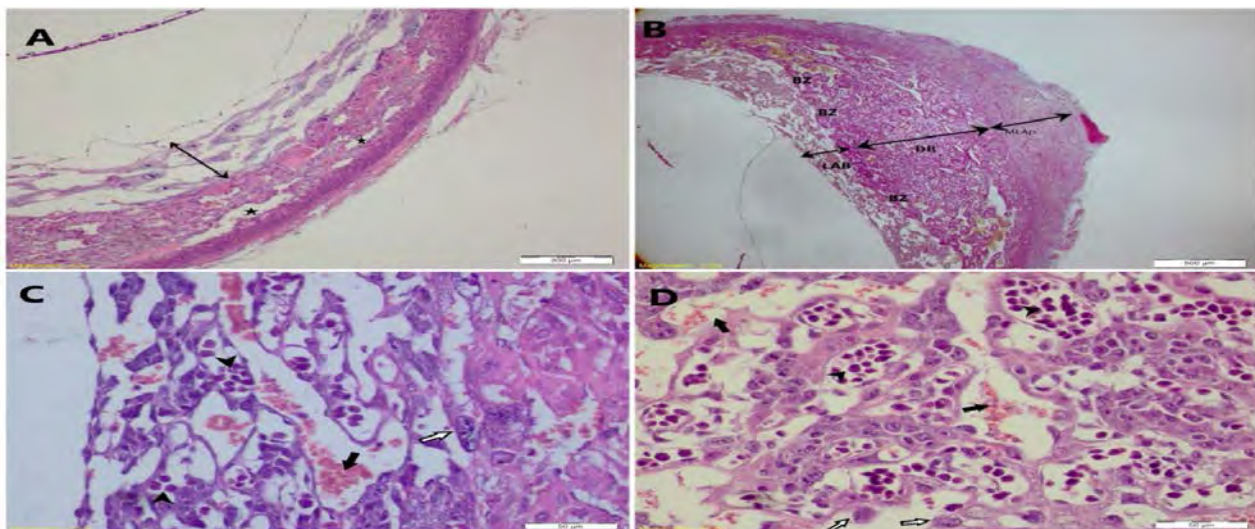


**Figure 5.** Tenth day of pregnancy. **A.** Lateral decidua areas. P-TGCs (double-sided arrow) and detachments start to form in the decidua (\*). Bar 200 µm. **B.** Mesometrial part. LAB: Labyrinth, BZ: Connection zone, DB: Decidua basalis, MLAp. Triple staining method. Bar 500 µm. **C, D.** The labyrinth part in development. Nucleated fetal erythrocytes (arrowhead), maternal blood spaces (black arrow), TGCs (white arrow). Hematoxylin-Eosin staining method. Bar 50 µm.

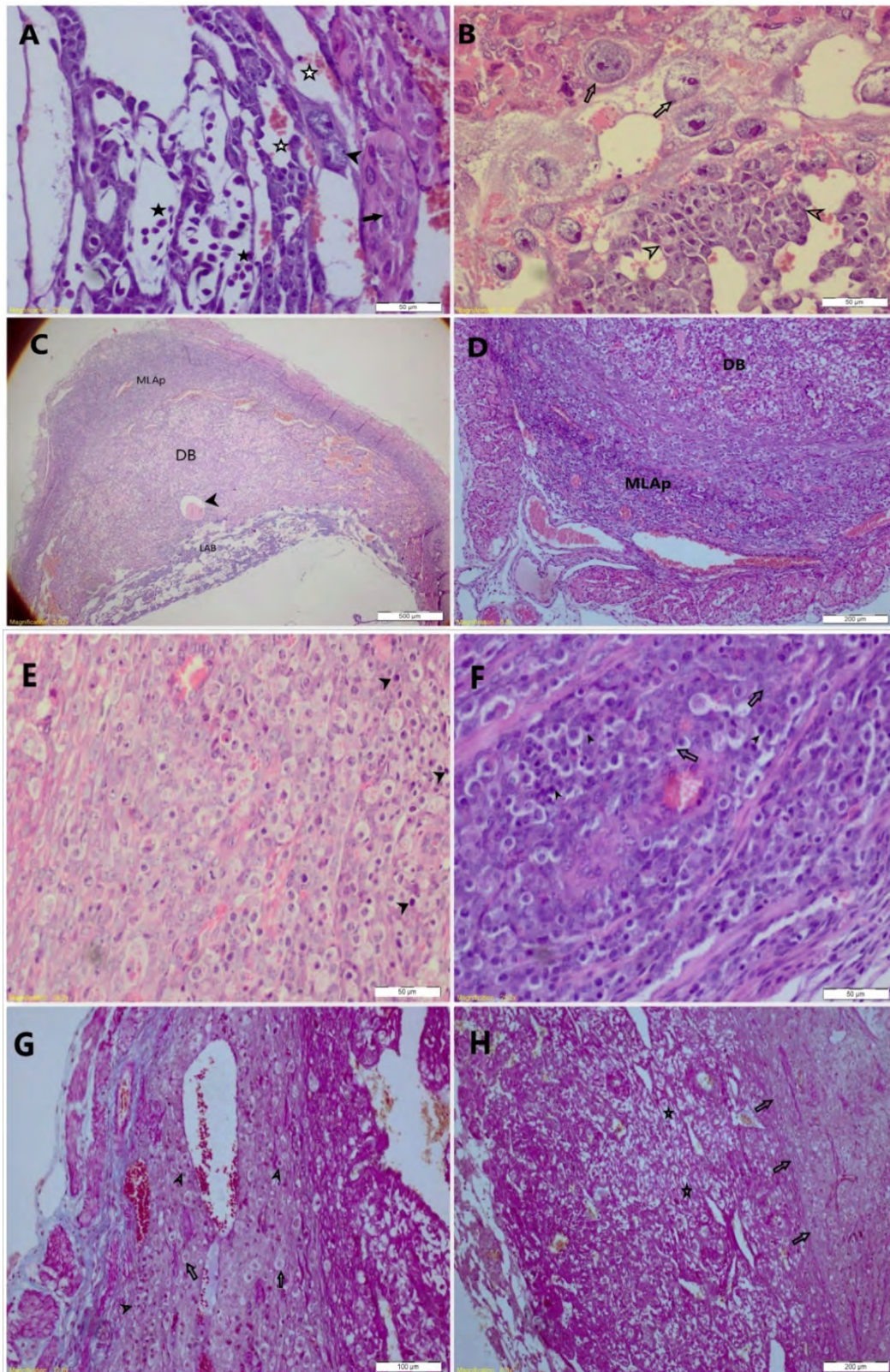


**Figure 6.** Tenth day of pregnancy.

**A.** Labyrinth-connection zone transition line. Erythrocytes with darkly stained nuclei (black stars) within fetal blood vessels. Nucleated erythrocytes (white stars) within maternal blood spaces. P-TGCs (arrowheads) bordering the labyrinth. Spongiotrophoblasts at the beginning of the junction zone. Hematoxylin-Eosin staining method. Bar 50  $\mu$ m. **B.** Labyrinth-connection zone transition line. P-TGCs (white arrow), Syncytiotrophoblasts (white arrowhead). Bar 50  $\mu$ m. **C.** Mesometrium. LAB: Labyrinth, DB: decidua basalis, MLap, main channel structure that brings blood to the labyrinth (arrowhead). Hematoxylin-Eosin staining method. Bar 500  $\mu$ m. **D.** MLap and DB (Decidua basalis) image. Bar 500  $\mu$ m. **E-F.** MLap (arrowheads), decidua (arrows). Hematoxylin-Eosin staining method. Bar 50  $\mu$ m. **G.** MLap. Decidua (white arrows), lymphocyte infiltrates (arrowheads). Triple staining method. Bar 500  $\mu$ m. **H.** Glycogen cells in decidua basalis (stars), end of decidua basalis, beginning of MLap (arrows). Hematoxylin-Eosin staining method. Bar 200  $\mu$ m.

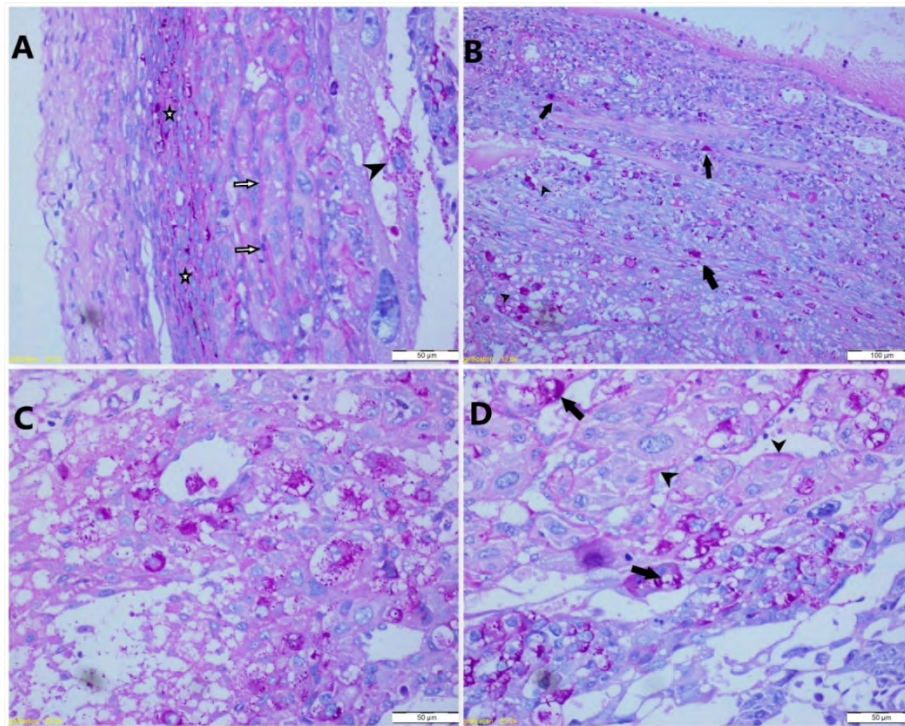


**Figure 7.** Tenth day of pregnancy. A) Decidua cells (white stars) showing strong PAS positivity in the antimesometrium, cell borders with decidua groups showing moderate reaction (white arrows), and P-TGC (black arrowhead) showing strong reaction in a granular manner. Bar 50  $\mu$ m. B) Mesometrium. MLap and decidua basalis transition zone. Glycogen cells with strong cytoplasmic reactions (black arrowheads). Cells giving PAS positivity within MLap, are thought to be uNK cells (black arrows). Bar 100  $\mu$ m. C) Glycogen cells showing strong cytoplasmic reaction. Bar 50  $\mu$ m. D) Labyrinth-connection zone-decidua basalis transition zone. Strongly reacting glycogen cells (arrows) Borders of decidua cell groups (arrowheads) showing moderate strength reaction. PAS staining method. Bar 50  $\mu$ m.

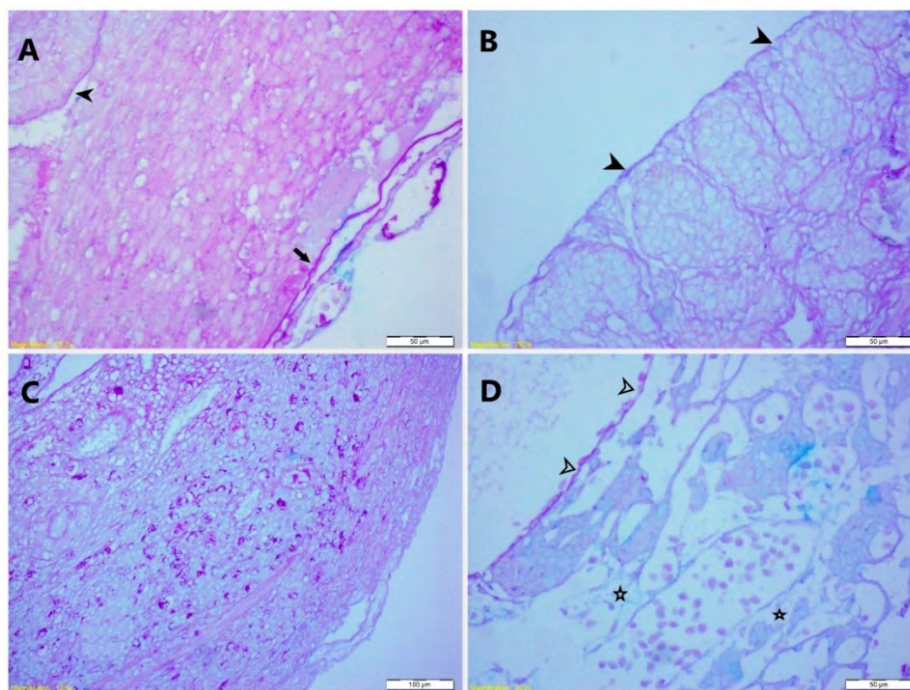


**Figure 8.** Tenth day of pregnancy. A) PAS (+) and AB (+) reaction (arrowhead) in the lamina epithelium of the antimesometrium and PAS positivity (arrow) at the border of the amniotic cavity. Bar 50  $\mu$ m. B) PAS (+) and AB (+) reaction in the serosa (arrowheads). Bar 50  $\mu$ m. C) General view of the decidua basalis-MLAP transition zone. Bar 100  $\mu$ m. D) Labyrinth. Amniotic cavity surface showing predominant PAS positivity (white arrowheads). Labyrinth areas (white stars) showing AB positivity. PAS-AB pH 2.5 staining method. Bar 50  $\mu$ m.

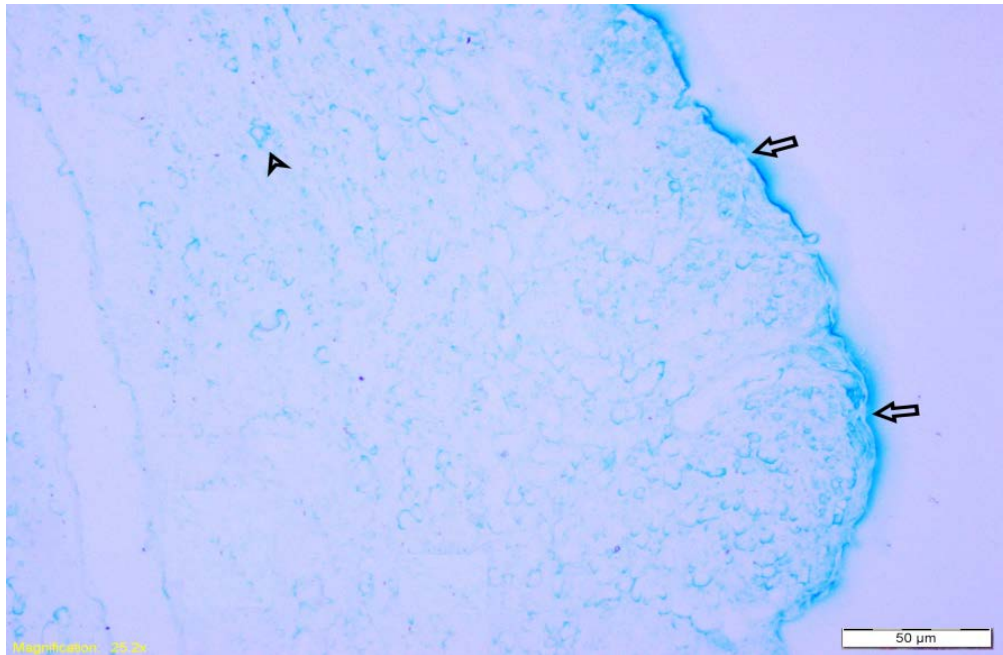


**Figure 9.** Tenth day of pregnancy. Strong AB pH 1.0 reaction in the serosa (arrows) and moderate reaction in the decidua (arrowhead). AB pH 1.0 staining method. Bar 50 µm.

**Seventeenth Day:** On the seventeenth day, a mature mouse placenta structure was observed. It was observed that the placenta consisted of four different main parts: decidua basalis, connection zone, labyrinth, and chorionic plate (Figure 10A, 10B). It was determined that decidua basalis extends from the mesometrium to the P-TGCs cells. It was noted that the presence of MLAp continued in the parts close to the mesometrium. Lymphocyte infiltrates were observed in this area (Figure 11A, 11B). Darkly stained spongiotrophoblast cells were detected in the junction zone and glycogen cells with light-colored foamy cytoplasm were detected between these cells (Figure 12A). At the border of the labyrinth, spongiotrophoblast cells were observed to make indentations in the labyrinth in the form of villus-like structures. In the part where the connection zone meets the decidua basalis, generally, single-row P-TGC cells bordering the basal zone were noted (Figure 12B, 12C, 12D). At the end of the connection zone, the presence of another fetal part, the labyrinth, was observed. In the labyrinth, there are generally fetal blood elements (Figure 13A, 13B), fetal endothelium, syncytiotrophoblasts (SynTC), and around them sinusoid trophoblastic giant cells (S-TGC) (Figure 13D, 13F), maternal blood pools and maternal erythrocytes circulating freely in these pools. was seen. Syncytiotrophoblasts were not clearly observed in all sections. The presence of a large channel was seen inside the labyrinth (Figure 13C, 13E). The presence of maternal erythrocytes was detected in this channel (Figure 13E). It was observed that channel trophoblastic giant cells (C-TGC) were lined up around this channel (Figure 13C, 13E). At the end of the labyrinth section, the chorionic plate section, facing the amniotic cavity, with dense vascular and channel structures in the center of the placenta, was seen (Figure 13F). In this section, channel trophoblastic giant cells and S-TGCs were

observed. Reichert's Membrane, which borders the placenta and extends as a thin line under the amnion and yolk sac layer that surrounds the entire placenta from the embryonal side, was noted (Figure 13H). This membrane was observed to be a homogeneous and avascular layer in all parts. The presence of a developed yolk sac with a basement membrane and an epithelium, spreading towards the amniotic cavity outside the placenta, was noted (Figure 13G, 13H).

The reactions observed with histochemical staining methods applied on the seventeenth day of pregnancy are given in Table 4.

On the seventeenth day, strong PAS positivity was observed on the basement membrane and epithelial surface of the yolk sac (Figure 14A). A very strong granular reaction was observed in the glycogen cells within the junction zone (Figure 14B). PAS-positive cells, thought to be uNK cells, were found in the MLAp-compatible region of the decidua basalis (Figure 14C, 14D). In the AB pH 2.5 staining method, moderate positivity was observed on the basement membrane of the yolk sac, and weak positivity was observed on the epithelial surface. In the PAS/AB pH 2.5 staining method, PAS was dominant on the yolk membrane and epithelial surface. In the AF staining method, medium strength positivity was observed on the yolk sac epithelial surface, vascular endothelium in the labyrinth, and vascular walls in the chorionic plate. In the AB pH 1.0 staining method, different strengths of reaction were observed in the serosa and glycogen cells. In the AB pH 0.5 staining method, a moderate reaction was detected on the serosa and yolk sac epithelial surface. In the AF/AB pH 2.5 staining method, AF positivity was observed on the basement membrane and epithelial surface of the yolk sac.

**Table 4.** Histochemical reactions on the seventeenth day of pregnancy.

	PAS	AB pH 2.5	PAS+AB	AF	AB pH 1.0	AB pH 0.5	AF+AB
Mesometrial decidua (Decidua basalis)	(+++)	-	PAS	(+++)	-	(++)	AF
Connection zone	(+++)	-	PAS	(++)	-	-	AF
Spongiotrophoblast							
Connection zone	(+++)	(+)	PAS	(+++)	-	(++)	AF
Glycogen Cells							
Labyrinth P-TGC	(++)	(+)	PAS	(++)	-	(+)	AF
Labyrinth	(+++)	Vessel walls, in the chorionic plate+ Basement embrane++, Epithelial surface +	PAS	(++)	(+)	(++)	AF
Yolk Sac	(+++)		PAS /AB	(+++)	(++)	(++)	(+++)
	Basement membrane and epithelial surface			Basement membrane epithelial surface			Basement membrane epithelial surface

None (-), Weak (+), Medium (++), Strong (+++).

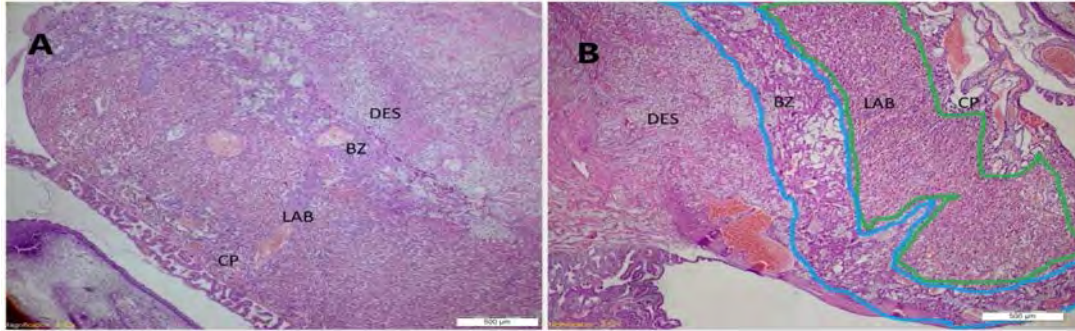


**Figure 10.** Seventeenth day of pregnancy. A-B. CP: Chorionic Plate, LAB: Labyrinth, BZ: Connection Zone, DES: Decidua basalis. Hematoxylin-Eosin staining method. Bar 500 µm.

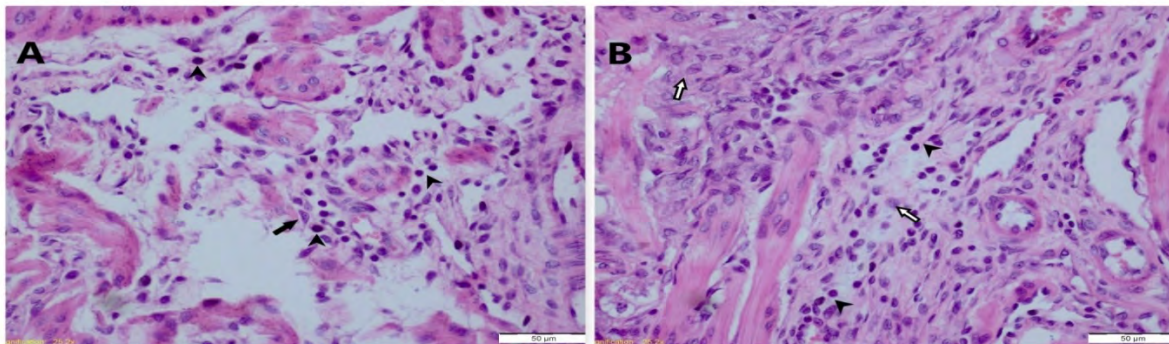


**Figure 11.** Seventeenth day of pregnancy. A-B. Lymphocyte infiltration (arrowheads), decidua cells (black and white arrows). Hematoxylin-Eosin staining method. Bar 50 µm.

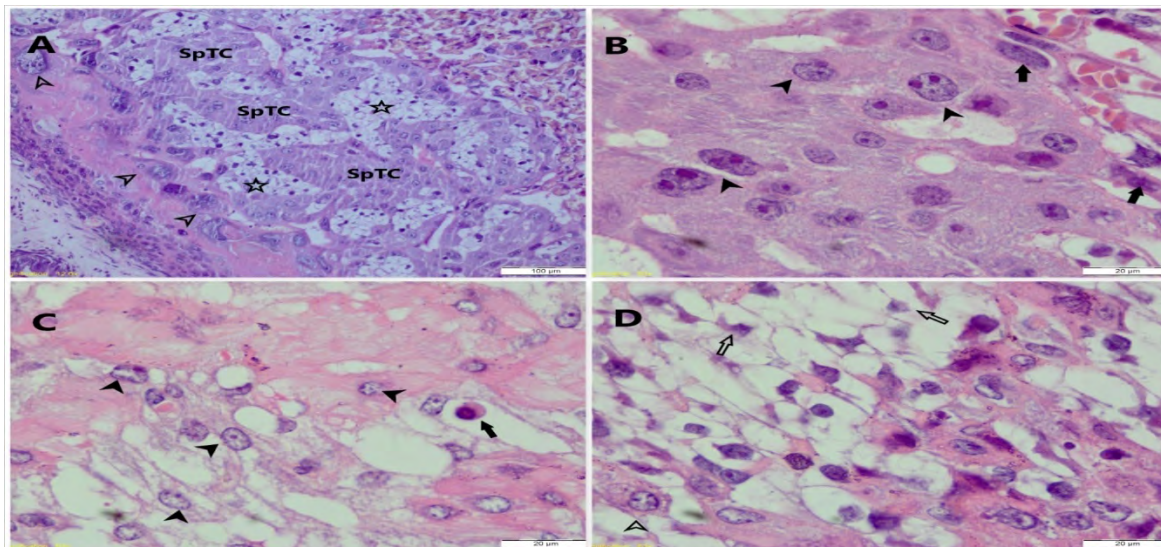


**Figure 12.** Seventeenth day of pregnancy. Junction zone of the placenta. A. SpTC: spongiotrophoblast cells, GlyC, glycogen cells (\*), TGC (arrowheads). Bar 100 µm. B. SpTC (arrowheads), S-TGC (arrows). Bar 20 µm. C. Decidua cells (arrowheads), plasma cells (arrow). Bar 20 µm. D. GlyC (white arrow), decidua cells (white arrowhead). Hematoxylin-Eosin staining method. Bar 20 µm.

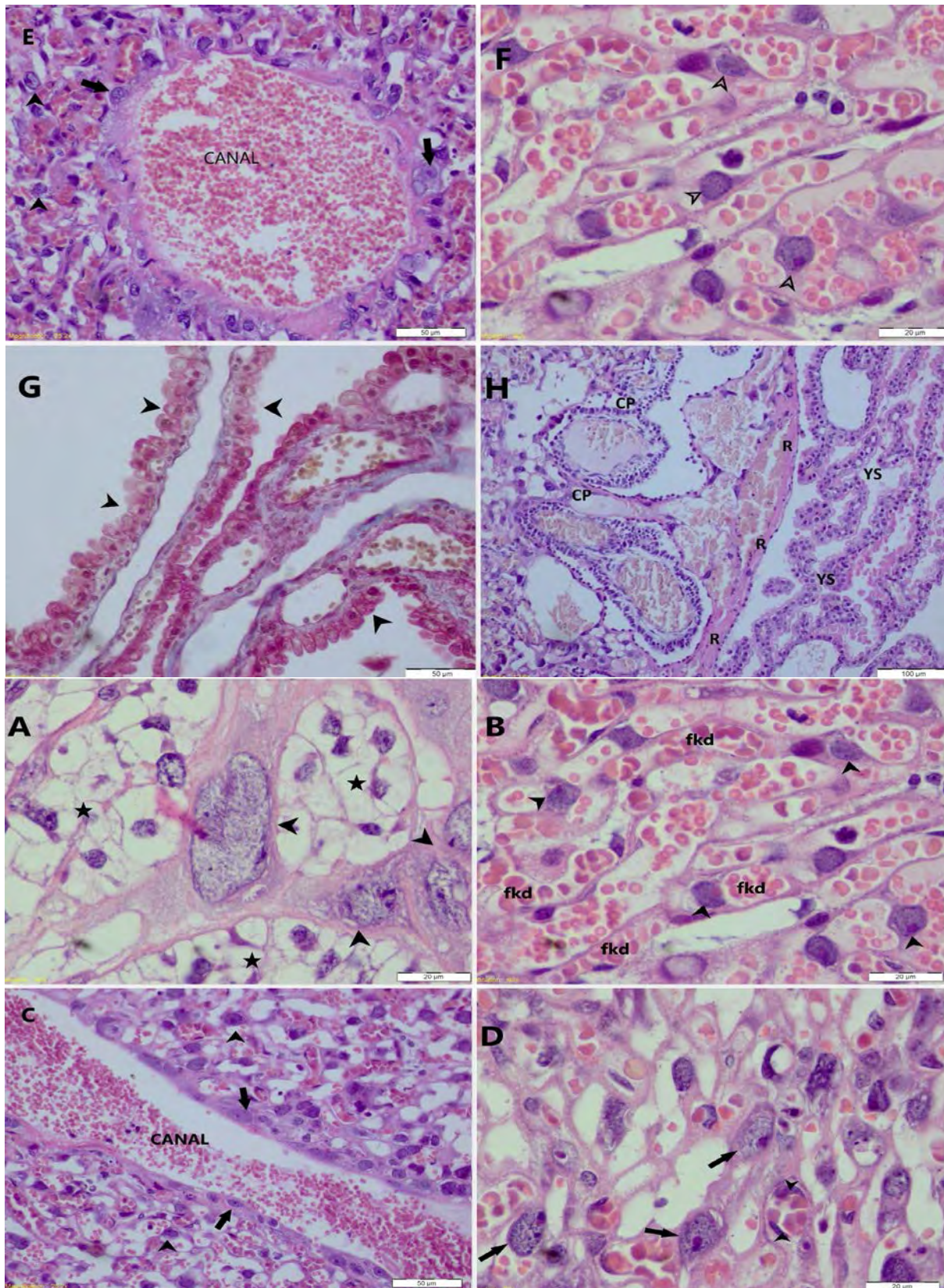


**Figure 13.** Seventeenth day of pregnancy. **A.** P-TGCs (arrowheads) located in the region limiting the fetal part, and GlyC communities (stars) located around it. Hematoxylin-Eosin staining method. Bar 20  $\mu$ m. **B.** Labyrinth. Fetal blood vessels (fkd) and S-TGCs (arrowheads) Hematoxylin-Eosin staining method. Bar 20  $\mu$ m. **C.** Channel structure in the labyrinth. C-TGCs (arrows), and S-TGCs (arrowheads) bordering the channel. Bar 50  $\mu$ m. **D.** Labyrinth S-TGCs (arrows), fetal endothelial cells (arrowheads). Hematoxylin-Eosin staining method. Bar 20  $\mu$ m. **E.** C-TGCs (arrows) on the labyrinth part canal wall. Bar 50  $\mu$ m. **F.** The labyrinth part. S-TGCs (arrows). Bar 20  $\mu$ m. **G.** Amniotic cavity, vitellus epithelial cells (arrowhead). Triple staining method. Bar 50  $\mu$ m. **H.** Chorionic plate region (CP) located at the end of the labyrinth section, Reichert's Membrane (R) limiting the chorionic plate, yolk sac (YS) in the amniotic cavity. Hematoxylin-Eosin staining method. Bar 100  $\mu$ m.

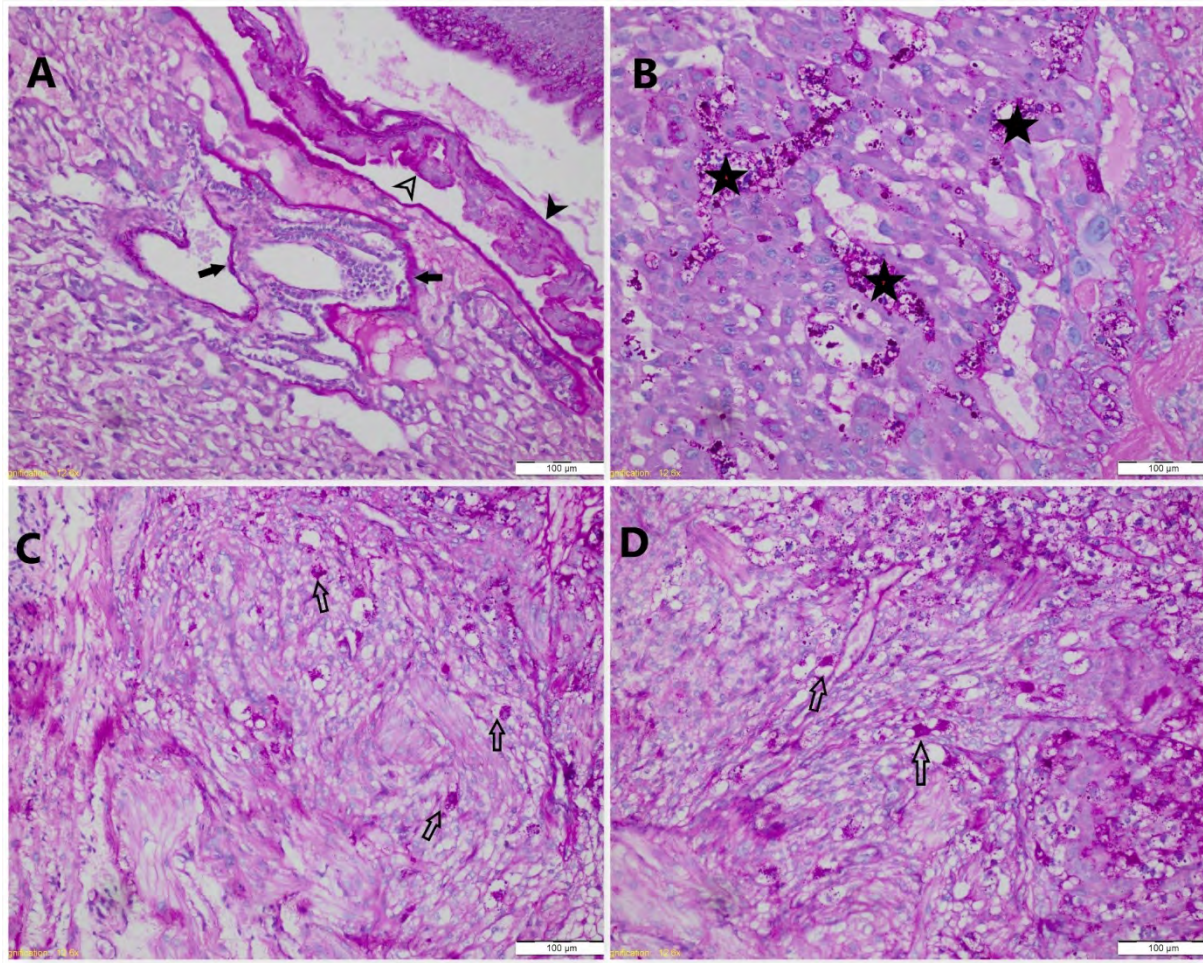


**Figure 14.** Seventeenth day of pregnancy. A) Strong PAS reaction on the yolk sac basement membrane (black arrowhead) and epithelial surface (white arrowhead). B) Glycogen cell populations showing a very strong granular PAS-positive reaction in the junction zone (\*). C-D) PAS+ cells (open arrows) thought to be uNK cells in the MLAp-compatible region. PAS staining method. Bar 100  $\mu$ m.

## Discussion

Edwards et al. (2014) reported in their study that the mouse uterus looked normal microscopically in the preimplantation period. They stated that the endometrium consists of the lumen epithelium of the uterus, gland epithelium, and stroma, circular and longitudinal myometrium surrounds the endometrium, and the outermost is the perimetrium.

In the presented study, it was observed that the histological structure of the uterus was generally preserved on the fourth day. It was determined that only some parts of the endometrium showed structural deterioration and some stromal cells began to differentiate structurally.

Studies report different findings regarding the day of implantation in mice. Enders and Blankenship (1999) stated that implantation occurred on the 4.5th day. Arvola (2001) states that it occurs on the 3.5th and 4th days, and in some studies, it occurs on the 4.5th and 5th days (Deb and Paria, 2006; Rossant and Cross, 2001; Watson and Cross, 2005). Deb and Paria (2006) state that the decidualization process is a response that occurs as a result of implantation, and that implantation is the initiator of the proliferation and

differentiation of uterine stromal cells. In another study, it was reported that the implantation area could be observed as early as the fifth day of pregnancy (Flores et al., 2014). In the presented study, no macroscopic or microscopic signs of implantation were found in the uterine samples taken on the fourth day of pregnancy, and no decidualization area was observed.

Sur et al. (2015) reported that decidualization begins in the mesometrial part where the implantation occurs as the implantation takes shape. It has been determined that, as decidualization progresses, parts of the mature structure of the placenta begin to form in the second and third weeks of pregnancy. The presented study observed that the placenta's main parts began to take shape from the tenth day of pregnancy, and the mature placenta structure was formed on the seventeenth day of pregnancy.

It is reported that fetal blood vessels begin to form towards the tenth day of pregnancy. These blood vessels widely invade the trophoblasts surrounding the maternal blood spaces, which can be observed on the 12th day of pregnancy (Enders and Blankenship, 1999). In this study, it was observed that on the tenth day of pregnancy, the labyrinth part began to form, maternal and fetal blood cells

could be clearly distinguished, and the maternal and fetal structures in the labyrinth were irregularly located and in the process of formation.

Flores et al. (2014) observed that on the 9th day of pregnancy, the antimesometrium, called the decidua capsularis, directly opposite the mesometrium, was considerably thinner than the mesometrium, but contained much more dense and dense cells and was much less vascularized. They also reported that nucleated fetal erythrocytes were clearly observed during this period. In the same study, when the 10th and 13th days of pregnancy were examined, it was stated that the placenta gained a mature placenta-like appearance, including the labyrinth zone, TGC zone, and spongiotrophoblast zone, and the decidua capsularis and the TGCs in between began to regress. In our study, histological findings similar to those of Flores et al. (2014) were obtained. On the tenth day of pregnancy, the antimesometrial decidua (decidua capsules) was considerably thinner and much less vascularized than the mesometrial decidua (decidua basalis). Its cellular density was much higher. Likewise, on the tenth day, fetal erythrocytes were nucleated and clearly distinguishable from maternal erythrocytes.

Edwards et al. (2014) stated that a large amniotic cavity, a prominent maternal decidua, and lumen residue were observed in the mouse uterus at day 9.5 of pregnancy. It has been stated that the MLAp part expands, is positioned between the myometrium, and divides the myometrium. It is reported that these changes occur in the mesometrial part, and the antimesometrial part is thinner. The same study stated that the mature placenta is generally formed on the 10.5th day of pregnancy, and the trophoblastic giant cell, spongiotrophoblast, and labyrinth layer can be clearly distinguished. It has been stated that TGCs terminate the labyrinth part, and nucleated fetal erythrocytes and nucleated maternal erythrocytes can be easily distinguished in the labyrinth part. It has been stated that the spongiotrophoblast layer is easily distinguished from the labyrinth, the amino space has widened considerably, and the lateral and antimesometrial decidua have begun to regress (Edwards et al., 2014). In this study, results supporting histological images were observed on the tenth day of pregnancy. It was observed that the labyrinth had begun to be established and was distinguished from the other layers, the antimesometrial layer was considerably thinner compared to the mesometrial part, the MLAp part was considerably enlarged, and nucleated fetal erythrocytes could be clearly seen in the labyrinth.

Harem and Alabay (2018) detected giant cells characterized by large nuclei and large cytoplasm, and glycogen cells clustered in the labyrinth, in the rat placenta on the fifteenth day of pregnancy. On the twentieth day, they reported that they observed giant cells, vacuolated cells in the decidual region, small basophilic cells with dark nuclei around the maternal and fetal vessels, and multinucleated trophoblast cells. The presented study found glycogen cells in the junction zone and occasionally in the decidua basalis on the seventeenth day. Giant cells were also observed in the labyrinth and the part bordering the labyrinth.

Edward et al. (2014) reported that in the mouse placenta, on the 15.5th day of pregnancy, the placenta was concentrated entirely in the antimesometrial part, and the decidua basalis and MLAp parts, which were evident in the previous days, started to regress. It is stated that the uterine cavity is completely re-epithelialized and becomes a residue. In the same study, it was reported that the placenta on the 19.5th day of pregnancy had all the histological features of a fully mature placenta, but some membranes began to appear dilated due to the last days of pregnancy. In this study, all histological layers of the mature mouse placenta could be observed on the seventeenth day of pregnancy. Consistent with the findings of the researchers, it was observed that the MLAp and decidua basalis part regressed and the placenta was located only in the antimesometrial part. On the seventeenth day, lamina epithelialis and uterine cavity were not observed.

**Histochemical Evaluations:** In a study conducted in rats (Mutluay, 2019), it was reported that basement membrane integrity continued and the basement membrane was PAS positive in samples taken on the fifth day of pregnancy. In the presented study, PAS positivity was observed in the basement membrane on the fourth day of pregnancy. Harem and Alabay (2018) applied PAS, AB pH 2.5, and PAS/AB staining methods to placenta samples from the sixth, tenth, fifteenth, and twentieth days of pregnancy in rats. In PAS histochemical staining, it was stated that positivity was observed in TGCs and other trophoblasts on the 10th day, and intense PAS positivity was observed in Gly-C and TGCs on the 15th and 20th days. In AB pH 2.5 staining, it was stated that on the tenth day, pale AB staining was again observed in the trophoblasts and the capsule surrounding the TGC. In PAS/AB pH 2.5 staining, it was reported that a faint AB positivity was observed in TGCs on the tenth day, PAS positivity was observed in TGCs on the fifteenth and twentieth days, and PAS positivity was also observed in trophoblasts on the twentieth day. In this study, intense PAS positivity was observed in Gly-C and TGCs, which is consistent with the study conducted on the tenth day of pregnancy. On the seventeenth day, intense PAS staining was observed in Gly-Cs. In AB pH 2.5 staining, a moderate reaction was observed in Gly-C and labyrinth, with a weak TGC on the tenth day, while an AB reaction was observed in Glyc-Cs on the seventeenth day. In a study investigating the effect of quercetin on placenta morphology in streptozotocin-stimulated diabetic rats (Erşahin et al., 2016), it was reported that as a result of PAS staining applied on the 21st day of pregnancy in control group rats, a high amount of PAS reaction was observed in the maternal part of the placenta in the control group and a low amount of PAS reaction was observed in the labyrinth zone. In this study, PAS reaction of varying intensity was observed in both the labyrinth and the maternal part in placenta samples from the seventeenth day of pregnancy.

It has been reported that PAS-positive areas are observed in the metrial region and decidua basalis in the later stages of pregnancy in mice (Sur et al., 2015). In our study, PAS-positive cells were found in the decidua basalis and mesometrial part on the seventeenth day of pregnancy.

It has been stated that glycogen cells give a positive reaction to PAS between days 6.5 and 12.5 of pregnancy (Tesser et al., 2010). In the presented study, Gly-C gave a positive reaction to PAS on the tenth and seventeenth days of pregnancy. Sur et al. (2015) reported in their study that Uterus Natural Killer Cells (uNK) cells showing intense PAS positivity were encountered in the decidua basalis in the middle and last days of pregnancy. It is stated that the number of these cells, which play a role in the restructuring of the endometrium and vessels during decidualization, is very high in the middle of pregnancy, and a significant decrease is observed towards the end of pregnancy (Sur et al., 2015). In the presented study, cells thought to be PAS-positive uNK were detected in the MLAp section on all gestational days studied. These cells were most dense on the tenth day of pregnancy.

It was reported that glycogen cells showed AB positivity after PAS-AB histochemical application applied after the decellularization process performed on the mouse placenta on the eighteenth and a half day of pregnancy (Barreto et al., 2019). In this study, the PAS positivity of glycogen cells was observed on the seventeenth day of pregnancy. Different AB pH 2.5 positivity levels were observed in glycogen cells in the junction zone.

As a result, this study determined the histological and histochemical characteristics of the mouse placenta during the fourth, tenth, and seventeenth days of pregnancy. This study will shed light on future studies and provide resources.

### Conflict of Interest

The authors stated that they did not have any real, potential, or perceived conflict of interest.

### Ethical Approval

This study was performed with the permission of the Experimental Animals Local Ethics Committee in Aydın Adnan Menderes University with (ADU HADYEK) 64583101/2016/017 approval number.

### Funding

This study was supported by Aydın Adnan Menderes University Scientific Research Fund with project number VTF-16004.

### Similarity Rate

We declare that the similarity rate of the article is 10 % as stated in the report uploaded to the system.

### \*Acknowledgment

This research article was summarized from a part of the first author's doctoral thesis.

### Author Contributions

Motivation/Concept: SK, ŞK  
Design: SK, ŞK

Control /Audit: ŞK  
Data Collection and/or Processing: SK  
Analysis and or Interpretation: SK, ŞK  
Literature Review: SK, ŞK  
Posted By: SK  
Critical Review: ŞK

### References

- Adams AD, Guedj F, Bianchi DW, 2020: Placental development and function in trisomy 21 and mouse models of Down syndrome: Clues for studying mechanisms underlying atypical development. *Placenta*, 89(1), 58-66.
- Arvola M, 2001: Immunological aspects of maternal-fetal interactions in mice. Doctoral thesis, comprehensive summary. *Acta Universitatis Upsaliensis*, 13-33.
- Barreto RSN, Romagnoli P, Fratini F, Mess AM, Miglino MA, 2019: Mouse placental scaffolds: a three-dimensional environment model for recellularization. *J Tissue Engin*, 10, 1-11.
- Chavatte-Palmer P, Tarrade A, 2016: Placentation in different mammalian species. In *Ann D'endocrin*, 77(2), 67-74.
- Culling CFA, Allison RT, Bar WT, 1985: Cellular Pathology Techniques. Butterworth & Co. (Publishers) Ltd. 113,217,232,233,238.
- Deb KF, Paria BC, 2006: Methodologies to study implantation in mice. In: Soares MJ, Hunt MJ (Eds) Placenta and Trophoblast. New Jersey Springer, 470p, 9-34.
- Edwards AK, Janzen-Pang J, Peng A, Tayade C, Carniato A, Yamada AT, Patricia DA, Tse D, 2014: Microscopic Anatomy of the Pregnant Mouse Uterus Throughout Gestation. In: Croy BA, Yamada AT, DeMayo FJ, Adamson SL(eds.), The Guide to Investigation of Mouse Pregnancy, Academic Press, Boston, 43-69.
- Enders AC, Blankenship TN, 1999: Comparative placental structure. *Advanced Drug Delivery Reviews*, 38(1), 3-15.
- Erşahin A, Hocaoglu M, Demire S, Cengiz F, 2016: Kuersetin, streptozotosin uyarımlı diyabetik sıçanlarda metabolik devreleri ve plasenta morfolojisini iyileştirmektedir. *Perin Derg*, 24(3), 147-55.
- Flores LE, Hildebrandt TB, Köhl AA, Drews B, 2014: Early detection and staging of spontaneous embryo resorption by ultrasound biomicroscopy in murine pregnancy. *Repr Biol Endocrin*, 12(1), 38.
- Furukawa S, Hayashi S, Usuda K, Abe M, Hagio S, Ogawa I, 2011: Toxicological pathology in the rat placenta. *J Toxicol Pathol*, 24(2), 95-111.
- Furukawa S, Kuroda Y, Sugiyama A, 2014: A Comparison of the histological structure of the placenta in experimental animals. *J Toxicol Pathol*, 27(1), 11-18.
- Hafez S, 2017: Comparative Placental Anatomy: Divergent Structures Serving a Common Purpose. *Progress in Molecul Biol Trans Sci*, 145, 1-28.
- Harem İŞ, Alabay B, 2018: Ratlarda gebeliğin değişik dönemlerinde trofoblastların özellikleri üzerinde histokimyasal ve immunohistokimyasal çalışmalar. *Harran Üniv Vet Fak Derg*, (Özel Sayı), 1-11.
- Johnson MH, Everitt BJ, 2018: Coitus and fertilization. In: Essential reproduction. John Wiley & Sons, United Kingdom, 145-160.
- Koç S, Kum S, 2022: Investigation of IgG, vimentin, CD45 distribution, and density in mouse placenta at different periods of pregnancy. *Turk J Vet Anim Sci*, 46,505-516.
- McGeady TA, Quinn PJ, FitzPatrick ES, Ryan MT, Kilroy D, Lonergan P, 2017: Fertilization In: Veterinary Embryology, University of Minnesota, 400, 26-100.

- Mutluay D, 2019: Preimplantasyon sürecinde sıçan uterus dokusunda meydana gelen değişikliklerin ışık mikroskopik düzeyde incelenmesi. *MAE Sağlık Bilimleri Enst. Derg*, 3(2), 43-53.
- Özer A, 2007: Veteriner Embriyoloji. Nobel Yayın Dağıtım, Ankara, 27-41.
- Rai A, Cross JC, 2014: Development of the hemochorial maternal vascular spaces in the placenta through endothelial and vasculogenic mimicry. *Develop Biol*, 387(2), 131-41.
- Rossant J, Cross JC, 2001: Placental development: lessons from mouse mutants. *Nature Rev Gen*, 2(7), 538.
- Sinowatz F, 2009: Fertilization. In: Hyttel P, Sinowatz F, Vejlsted M, Betteridge K (eds), *Essentials of domestic animal embryology*. Elsevier Health Sciences, Canada, 56-68.
- Sur E, Öznurlu Y, Özaydin Y, Çelik İ, Aydın İ, Kadyralieva N, 2015: Gebe farelerde desidua bazalis dokusundaki PAS-pozitif uterus doğal katil hücrelerinin dağılımı. *Kafkas Univ Vet Fak Derg*, 21(3), 405-411.
- Tesser RB, Scherholz PLA, Nascimento L, Katz SG, 2010: Trophoblast glycogen cells differentiate early in the mouse ectoplacental cone: putative role during placentation. *Histochem Cell Biol*, 134, 83-92.
- Tewari V, Tewari A, Bhardwaj N, 2011: Histological and histochemical changes in placenta of diabetic pregnant females and its comparison with normal placenta. *Asian Pacific J Trop Dis*, 1(1), 1-4.
- Watson ED, Cross JC, 2005: Development of structures and transport functions in the mouse placenta. *Physiol*, 20, 180-93.
- Wu D, Xu J, Lei J, McLane M, Zijl PC, Burd I, 2018: Dynamic glucose enhanced MRI of the placenta in a mouse model of intrauterine inflammation. *Placenta*, 69, 86-91.
- Yu Q, Qiu Y, Wang X, Tang J, Liu Y, Mei L, Li M, Yang M, Tang L, Gao H, Zhang Z, Xu W, He Q, 2018: Efficient siRNA transfer to knock down a placenta-specific lncRNA using RGD-modified nanoliposome: A new preeclampsia-like mouse model. *Inter J Pharm*, 546(1-2), 115-24.
- Zhu H, Xu X, Shi X, Feng Y, Xiong Y, Nan Y, Zhang C, Gao L, Chen Y, Xu D, Wang H, 2019: Activation of autophagy inhibits cadmium-triggered apoptosis in human placental trophoblasts and mouse placenta. *Environ Poll*, 254(PtA), 112991.